HUMAN GENE THERAPY 22:567–575 (May 2011)
© Mary Ann Liebert, Inc.
DOI: 10.1089/hum.2010.140

AAV Delivery of Wild-Type Rhodopsin Preserves Retinal Function in a Mouse Model of Autosomal Dominant Retinitis Pigmentosa

Haoyu Mao,[1] Thomas James, Jr.,[1] Alison Schwein,[1] Arseniy E. Shabashvili,[1] William W. Hauswirth,[1,2] Marina S. Gorbatyuk,[1,3] and Alfred S. Lewin[1]

Abstract

Autosomal dominant retinitis pigmentosa (ADRP) is frequently caused by mutations in *RHO*, the gene for rod photoreceptor opsin. Earlier, a study on mice carrying mutated rhodopsin transgenes on either *RHO*+/+ or *RHO*+/– backgrounds suggested that the amount of wild-type rhodopsin affected survival of photoreceptors. Therefore, we treated P23H *RHO* transgenic mice with adeno-associated virus serotype 5 (AAV5) expressing a cDNA clone of the rhodopsin gene (*RHO301*) that expressed normal opsin from the mouse opsin promoter. Analysis of the electroretinogram (ERG) demonstrated that increased expression of *RHO301* slowed the rate of retinal degeneration in P23H mice: at 6 months, a-wave amplitudes were increased by 100% and b-wave amplitudes by 79%. In contrast, nontransgenic mice injected with AAV5 *RHO301* demonstrated a decrease in the ERG, confirming the damaging effect of rhodopsin overproduction in normal photoreceptors. In P23H mice, the increase in the ERG amplitudes was correlated with improvement of retinal structure: the thickness of the outer nuclear layer in *RHO301*-treated eyes was increased by 80% compared with control eyes. These findings suggest that the wild-type *RHO* gene can be delivered to rescue retinal degeneration in mice carrying a *RHO* mutation and that increased production of normal rhodopsin can suppress the effect of the mutated protein. These findings make it possible to treat ADRP caused by different mutations of *RHO* with the expression of wild-type *RHO*.

Introduction

Retinitis Pigmentosa (RP) is a neurodegenerative disorder with the prevalence of 1 in 4,000 and almost 1.5 million patients in the world (Phelan and Bok, 2000; Hartong *et al*., 2006; Daiger *et al*., 2007). It is characterized by apoptotic death of rod photoreceptor cells. There are three forms of RP: autosomal dominant RP (ADRP), autosomal recessive RP, and X-linked RP, with ADRP accounting for 40% of clinical cases. Although the pathological progression is variable in different individuals diagnosed with ADRP, the primary symptoms are gradual loss of vision in the dark followed by loss of peripheral vision. Eventually, central vision is diminished by cone-cell degeneration late in the disease course (Van Soest *et al*., 1999; Farrar *et al*., 2002).

Pioneering work by geneticists and ophthalmologists over the past two decades has identified mutations in 20 genes that lead to ADRP, paving the way for the possible gene-specific treatments of this complex disease (Bok, 2007). Rhodopsin is encoded by one of these genes (*RHO*), and mutations in *RHO* are associated with over 25% of ADRP cases (Daiger *et al*., 2007). The first identified *RHO* mutation, P23H (proline 23 substituted by histidine), is associated with 12% of ADRP patients in the United States (Dryja *et al*., 1990; Van Soest *et al*., 1999; Daiger *et al*., 2007). Different models have been proposed for the mechanism of photoreceptor death resulting from *RHO* mutations, and these vary based on the amino acid residue affected (Dryja *et al*., 2000; Stojanovic *et al*., 2003; Lewis and Kono, 2006). To study the underlying pathology of ADRP, several P23H transgenic animal models, including mouse, rat, fly, and frog models, have been developed (Olsson *et al*., 1992; Roof *et al*., 1994; Organisciak *et al*., 2003; Galy *et al*., 2005; Gorbatyuk *et al*., 2005b; Tam and Moritz, 2006). In the rat model, Saito and colleagues have shown that P23H rhodopsin exhibits delayed dephosphorylation, and they suggest that abnormal levels of cytosolic Ca^{2+} are responsible for cell death (Saito *et al*., 2008).

Protein misfolding caused by the P23H mutation may also contribute to pathogenesis by interfering with the transport or function of normal rhodopsin and by initiating endoplasmic reticulum (ER) stress (Illing *et al*., 2002; Lin *et al*.,

[1]Department of Molecular Genetics and Microbiology, University of Florida, Gainesville, FL 32610.
[2]Department of Ophthalmology, University of Florida, Gainesville, FL 32610.
[3]Current address: Department of Cell Biology and Anatomy, University of North Texas Health Science Center, Ft. Worth, TX 76107.

2007). One point of discussion concerns whether *RHO* mutations cause photoreceptor death by a toxic gain-of-function mechanism or by a dominant negative mechanism. Stimulation of unregulated phototransduction would suggest the former, but photoreceptor damage in P23H transgenic frogs does not require activation of transducin, suggesting that phototransduction is not required for rod cell death (Tam and Moritz, 2006). Study of the GHL allele of rhodopsin in transgenic mice (the H in this case represents P23H) suggests that the mutation behaves in a dominant negative fashion: the rate of retinal degeneration observed in the presence of one wild-type endogenous allele (*RHO*+/–) was significantly greater than when two normal copies were present (*RHO*+/+) (Frederick *et al*., 2001).

Animal models of ADRP have also been useful in testing therapies for RP. Despite the complexity and genetic heterogeneity of ADRP, several research groups have been involved in the development of a gene therapy in animal models. Our group and two others have explored "a cut and replace" therapy using RNA interference (RNAi) or catalytic RNA enzymes (ribozymes) (Lewin *et al*., 1998; Sullivan *et al*., 2002; Gorbatyuk *et al*., 2005a, 2007b, 2008; Kiang *et al*., 2005). Both allele-dependent and allele-independent strategies have been attempted. For the allele-dependent method, specific ribozymes or small interfering RNAs (siRNAs) were designed to silence the mutant gene, but leave the original mRNA uncut to obtain a knockdown of the mutant rhodopsin in ADRP animal models. Some of these studies showed rescue of retinal structure and function in the animal models (Lewin *et al*., 1998; Gorbatyuk *et al*., 2004). In contrast, an allele-independent approach was designed to suppress expression of both mutant and wild-type genes in order to treat ADRP patients with different mutations (Sullivan *et al*., 2002; Cashman *et al*., 2005; Kiang *et al*., 2005; Tessitore *et al*., 2006; Gorbatyuk *et al*., 2007a,b, 2008). In this case, a gene for wild-type rhodopsin that is resistant to the RNA knockdown agent is supplied in the same vector. This approach has led to rescue of vision when tested in ADRP mice (Palfi *et al*., 2006; O'Reilly *et al*., 2008; Smith *et al*., 2009).

In earlier work, we demonstrated that gene transfer of siRNA301, which is specific for mouse *RHO*, to photoreceptors leads to long-term rescue of photoreceptors in rats bearing a mutant mouse *RHO* transgene (Gorbatyuk *et al*., 2007b). We began the present studies to optimize the expression of an allele of *RHO* (*RHO301*) that encodes the normal protein, but is resistant to cleavage by this siRNA. In the course of these experiments, we determined that the increased production of normal rhodopsin rescued photoreceptor function in P23H *RHO* mice, suggesting that gene therapy with normal gene is possible for treatment of many different ADRP mutations affecting rhodopsin.

Materials and Methods

Cloning of the RHO301 *gene*

The mouse *RHO* (GenBank accession number BC013125) cDNA we used contained a 109-bp 5′-untranslated region (UTR) and a 159-bp 3′-UTR. It also contains five silent mutations to eliminate the siRNA301 recognition site (wild-type: CTTCCTCACGCTCTACGTC to *RHO301*: CTTCTTAACC TTGTACGTC).The production of the opsin protein was confirmed by immunohistochemistry of 293 cells transfected with a plasmid expressing *RHO301* from the cytomegalovirus immediate-early promoter (data not shown). For *in vivo* studies, *RHO301* was embedded in an adeno-associated virus (AAV) vector under the control of a mouse proximal opsin promoter (Flannery *et al*., 1997). Recombinant vector then was packaged in AAV serotype 5 (AAV5), resulting in a final titer of 2×10^{12} viral genomes/ml (Zolotukhin *et al*., 2002).

Animal model

All experimental procedures with mice were approved by the University of Florida Institutional Animal Care and Use Committee in accordance with the NIH Guide for Care and Use of Laboratory Animals and the ARVO Statement for the Use of Animals in Ophthalmic and Vision Research. P23H transgenic mice (line 37) contains a human P23H *RHO* transgene comprised of the entire rhodopsin gene transcriptional unit plus 4.2 kb of upstream and 8.4 kb of downstream DNA. Founder P23H *RHO* mice (on an FVB background) were backcrossed with C57BL/6J mice for 10 generations to obtain human transgenic mice on a uniform B6 genetic background. This line contains an equal number of copies of the human *RHO* transgene and the endogenous mouse *RHO* gene (Supplementary Fig. S1; supplementary data are available online at www.liebertonline.com/hum). As the wild-type animals, we used C57BL/6J mice that were purchased from Jackson Laboratories (Bar Harbor, ME). Consistent with the nomenclature of Dryja and colleagues, and to indicate that the mice have two copies of the endogenous *RHO* gene, we term these mice hP23H *RHO*+/–, m*RHO*+/+(Dryja *et al*., 1990; Olsson *et al*., 1992). All mice were housed in a 12-hr light/12-hr dark cycle under specific pathogen-free conditions.

Subretinal AAV injections were performed as described by Timmers *et al*. (2001). Wild-type and P23H *RHO* mice were injected at postnatal day 15 (P15). For this purpose, mice were anesthetized by ketamine/xylazine injection. Pupils were dilated with one drop of 1% atropine sulfate and 2.5% phenylephrine. Right eyes were injected in the superior hemisphere with 1 μl of AAV *RHO301* (2×10^9 vector genomes), and left eyes were kept as untreated controls. For injection controls, other mice were injected with AAV of the same titer expressing green fluorescent protein (GFP) from the mouse opsin promoter.

RNA analysis

Total RNA was extracted from retinas of three P23H mice treated with AAV-*RHO301* in their right eyes and uninjected in their left eyes. TRIzol reagent (Invitrogen, Carlsbad, CA) was used to isolate RNA from fresh retinas according to the manufacturer's procedure. Extracted RNA samples were treated with RNase free DNase I (Ambion, Austin, TX) to remove DNA contamination. RNA concentration was estimated by A260 using a NanoDrop N-1000 spectrophotometer (NanoDrop, Wilmington, DE). Human *RHO*, mouse *RHO* and mouse *RHO301* mRNA were converted into cDNA by RT-PCR with a first-strand cDNA synthesis kit (GE Healthcare, Piscataway, NJ). Gene-specific primers were used for reverse transcription of mouse and human *RHO* and β-actin: 5′-TTCTCCCCGAAGCGGAAGTT-3′ (*RHO* exon 2), 5′-TGGCCATCTCCTGCTCGAAGTC-3′ (β-actin). Forward PCR primers were: 5′-CCATGGCAGTTCTCCATGCT-3′ for

both human and mouse *RHO* exon 1 and 5′-TGAG ACCTTCAACACCCCAGCC-3′ for β-actin. After PCR amplification, PCR products were purified using a GenElute PCR Clean-Up Kit (Sigma–Aldrich, St. Louis, MO), and *RHO* PCR products were digested with the endonuclease *Mse*I (Promega, Madison, WI), which does not cleave within the human P23H and mouse *RHO* PCR products, but does cleave within *RHO301*. Treatment of these PCR products gave one band of 353 bp in the samples of uninjected retinas. The *RHO301* PCR digested with *Mse*I gave two bands of 70 bp and 283 bp. After digestion, PCR products from left and right eyes were loaded on 12% polyacrylamide gels run in Tris-borate EDTA buffer for measurement of both *RHO* PCR products and β-actin PCR products. SYBR Green (Invitrogen) was used to stain PCR product bands. The intensity of each band was detected with a scanner and analyzed using "Quantity One" software (Bio-Rad, Hercules, CA) to quantify the volume of each band of interest. Expression of *RHO* mRNA was normalized based on β-actin content.

Protein extraction and immunoblots

At 1 month after injection, three P23H mice or wild-type mice were euthanized by carbon dioxide inhalation, and the retinas were dissected. Protein extracts of retinas were prepared by sonication in electrophoresis sample buffer (Laemmli, 1970). Concentration of total retinal proteins from each sample was detected by the Pierce BCA protein assay kit (Thermo Scientific, Rockford, IL). For immunoblotting, 20 μg of total protein from each sample was loaded on 12% sodium dodecyl sulfate–polyacrylamide gels run in Tris-glycine buffer. Proteins were transferred to polyvinylidene fluoride membranes by iBlot dry blotting system (Invitrogen). After transferring, the blots were treated with either a monoclonal antibody against an N-terminal bovine rhodopsin fragment (B6-30) or a monoclonal antibody against the C-terminus of mouse rhodopsin (1D4). The second antibody detects all rhodopsin proteins, including the P23H *RHO*. However, it is possible that B6-30 might have a lower affinity to P23H opsin due to the P23H mutation. For secondary antibodies, we used infrared dye-tagged anti-mouse (for rhodopsin) and anti-rabbit (for β-actin) IgG from LI-COR Biosciences (Lincoln, NE). Stained blots were scanned and analyzed for intensity by using the LI-COR Odyssey scanner and Odyssey analysis software. Levels of rhodopsin protein were normalized to the endogenous β-actin.

Electroretinography (ERG)

At 1, 2, 3, and 6 months following subretinal injection, mice were analyzed by simultaneous full-field ERG. For ERG, mice were dark-adapted overnight, then anesthetized with ketamine/xylazine, and their eyes dilated in dim red light with 2.5% phenylephrine solution. Small contact lenses with gold wire loops were placed on each cornea with a drop of 2.5% methylcellulose to maintain corneal hydration. A silver wire reference electrode was placed subcutaneously between the eyes, and a ground electrode was placed subcutaneously in a hind leg. Responses from both eyes were recorded simultaneously using a UTAS-E 2000 Visual Electrodiagnostic System (LKC Technologies, Gaithersburg, MD). Scotopic ERGs, which primarily measure rod function, were elicited with 10-msec flashes of white light at −30, −20, −10, and 0 dB with appropriate delay between flashes. Five to 10 scans were averaged at each light intensity. The a-wave amplitudes were measured from baseline to the peak in the cornea-negative direction, and b-wave amplitudes were measured from cornea-negative peak to major cornea-positive peak. The results from each group of mice were averaged, and the means were compared statistically by using Student's *t* test for paired data, when comparing treated and control eyes from the same mice. For comparison of the mean amplitudes of multiple groups, we used ANOVA.

Histological analysis

For morphometric analysis, the retinas were fixed and prepared for plastic sectioning after perfusion in 2% paraformaldehyde plus 2.5% glutaraldehyde. Dissected tissues were postfixed in 1% osmium tetroxide at 4°C for 4 hr and then maintained in 0.1 *M* cacodylate buffer overnight. After dehydration, tissues were embedded in an epoxy resin. Tissue sections (1 μm) were made along the vertical meridian through the optic disc and stained with toluidine blue. The thickness of the outer nuclear layer (ONL) was measured at five equally spaced superior loci and five inferior loci using the MBF Stereo Investigator (MicroBrightField, Inc., Williston, VT) connected to a Zeiss microscope. Ten measurements were averaged at each site with system software by an operator who was unaware of the identity of the samples. The distribution of the ONL thickness of superior and inferior retina was determined by the mean thickness from each section. Analysis was described by Faktorovitch *et al*. (1990). Differences between the ONL thickness of left control eyes and right treated eyes were analyzed by using Student's *t* test for paired samples. A p value of <0.05 was considered significant.

Quantification of apoptosis

Six P23H transgenic mice were injected in their right eyes with AAV-*RHO301*on P15; 1 month later, the retinas from both eyes were extracted to detect the apoptotic cells by a nucleosome release assay, using the cell death detection ELISA kit (Roche Diagnostics, Indianapolis, IN). In brief, based on the manufacturer's protocol, each retinal sample was placed in 200 μl of lysis buffer on ice. *RHO301*-injected and uninjected retinas were homogenized for 3 sec with a tissue homogenizer (Polytron; PT1200). Insoluble material was sedimented by centrifugation at full speed in a microcentrifuge, and 10 μl of the supernatant was diluted 1:100 in lysis buffer. Twenty microliters of the final solution was used to measure the nucleosome release.

Results

Expression of AAV-delivered RHO301

We constructed the *RHO301* allele by introducing five silent mutations into a normal mouse *RHO* cDNA clone to eliminate the cleavage site for a previously designed siRNA (Gorbatyuk *et al*., 2007b, 2008). The gene was delivered by subretinal injection of an AAV2 vector pseudotyped with AAV5 capsids on P15. Expression was driven by the mouse opsin proximal promoter (Supplementary Fig. S2). To confirm the expression of *RHO301* in P23H retinas, we analyzed the mRNA level of the transferred gene 1 month following

subretinal injection with AAV-*RHO301*. To distinguish *RHO301* mRNA from endogenous mouse *RHO* mRNA and the mRNA produced by the human P23H transgene, we used a restriction site that was created in the *RHO301* allele by the silent mutations. Total amplified PCR products were digested with *Mse*I, and digestion products were normalized to β-actin PCR amplification products from the same samples (Fig. 1A). Compared with rhodopsin mRNA levels in untreated left eyes, we obtained an almost twofold increase of total *RHO* mRNA in treated right eyes (Fig. 1B), indicating the successful delivery and expression of *RHO301* in right eyes ($p < 0.005$).

Proteins were also extracted from P23H retinas of mice 1 month after subretinal injection, and expression of rhodopsin was detected by immunoblot using mouse anti-rhodopsin monoclonal antibodies 1D4, which recognizes a C-terminal epitope, and B6-30, which recognizes an N-terminal epitope (Fig. 1C and D). For data analysis, the rhodopsin band was normalized using the intensity of the endogenous β-actin band. A 58% increase of monomer protein level and a

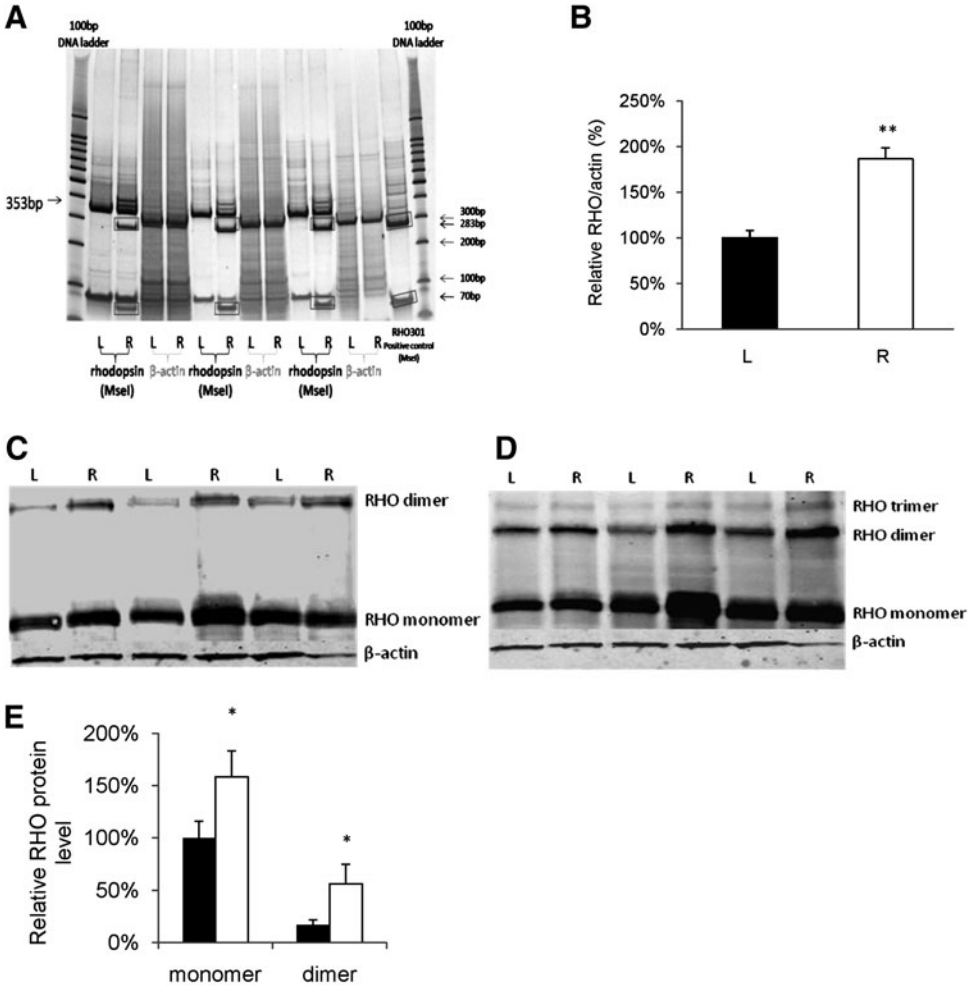

FIG. 1. Increased expression of rhodopsin following AAV delivery of *RHO301*. Expression of *RHO* mRNA was elevated nearly twofold by AAV5-*RHO301* gene transfer in P23H transgenic mice ($p < 0.005$). (**A)** Image of a polyacrylamide gel with *Mse*I digestion products of PCR products from left uninjected and right injected eyes of three randomly selected mice. To differentiate the *RHO301* transcript from endogenous *RHO* mRNA, total RNA extraction was amplified by specific rhodopsin primers, and PCR products were digested by *Mse*I. Both mouse *RHO* and human transgenic P23H *RHO* products were uncut by *Mse*I (353 bp), but *RHO301* PCR products were digested into 283-bp and 70-bp fragments (rectangular boxes) in right, *RHO301*-injected eyes (labeled R), but not in uninjected left eyes (labeled L). *Mse*I-digested *RHO301* PCR products were applied as a positive control. A 100-bp DNA ladder was used as size marker. (**B)** Densitometric quantification of the scanned gel. *RHO* PCR products were normalized by the intensity of the endogenous β-actin PCR product. The ratio of the intensity of the 353-bp fragment to the β-actin fragment in uninjected left eyes (black bar) was set to 100%, and the ratio of injected right eyes (white bar) was significantly increased (**$p < 0.005$). (**C** and **D**) Elevation of rhodopsin protein levels in eyes treated with AAV-*RHO301*. Western blot analysis of rhodopsin protein production in three P23H mice injected with *RHO301* in their right eyes using 1D4 (C) or B6-30 (D) monoclonal antibodies. (**E**) Densitometric quantification of the blot in panel C reveals an elevated production of opsin protein in injected right eyes (white bars) compared with uninjected left eyes (black bars). The data were normalized to endogenous β-actin, and the ratio of intensity of the untreated opsin monomer was set as 100% (*$p < 0.05$).

threefold increase in the dimer was found in the *RHO301*-injected eyes ($p < 0.05$) (Fig. 1E). Similar results were found using both monoclonal antibodies. Under native conditions, rhodopsin forms dimers and higher-order species in rod outer segments (Fotiadis *et al.*, 2003). As we saw no increase in endogenous mouse *RHO* transcripts (data not shown), we conclude that the elevation in opsin protein is attributable to expression of *RHO301* rather than to increased survival of rods at this early stage (6 weeks of age).

*Rescue of retinal function in AAV-*RHO301*-treated P23H eyes in mouse and rat models*

To assess retinal function in treated eyes, the full-field electroretinogram (ERG) was measured in dark-adapted mice at increasing intervals following injection. To control for the impact of injection (Wen *et al.*, 1995), we injected additional P23H transgenic mice with AAV5-expressing GFP from the mouse opsin promoter. Analysis of ERG amplitudes showed that there was no difference in retinal function between uninjected and GFP-injected mice over the course of 3 months (Fig. 2A). However, the a-wave and b-wave amplitudes for *RHO301*-injected eyes were higher compared with those for GFP-injected animals at 1 month after injection. At 3 months post injection, we observed an almost twofold increase for both a-wave and b-wave amplitudes in the *RHO301*-injected eyes versus the GFP-injected contralateral eyes ($p < 0.05$).

Over a longer time course, *RHO301* gene transfer consistently improved both the a-wave and b-wave responses of P23H mice compared with those of untreated control eyes (Fig. 2B and C). At 6 months post injection, there was a 2.8-fold increase of a-wave amplitude in injected eyes compared with untreated eyes ($p < 0.005$). Although the a-wave amplitudes from the treated eyes declined gradually compared with the value at 1 month post injection, they remained relatively constant (around 200 μv) from 2 months to 6 months (Fig. 2B). Moreover, there was significant increase in the latency (implicit time) of the a-wave in untreated P23H retinas. (Implicit time was measured from the light flash to the negative peak of the a-wave.) In *RHO301*-injected P23H mice, the implicit time of the injected right eyes was shorter than that of the uninjected left eyes at 3 months and 6 months (Supplementary Fig. S3A). The b-wave amplitudes of *RHO301*-treated eyes were also substantially improved (sixfold) compared with those of untreated P23H eyes (Fig. 2B)

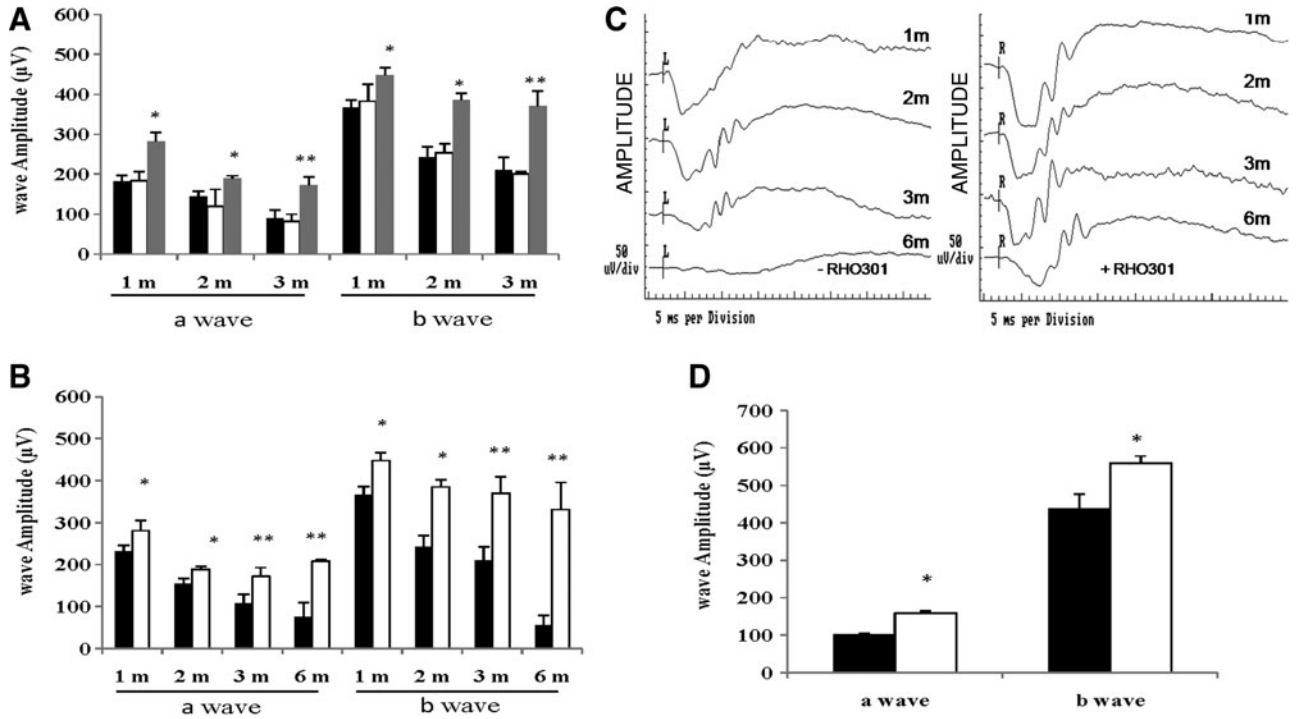

FIG. 2. Increased expression of rhodopsin protects P23H retinas in both P23H mice and rats. Both a-wave and b-wave amplitudes of scotopic (dark-adapted) full-field ERG were evaluated in nine P23H mice injected with AAV-*RHO301* (gray bars) and compared with nine mice injected with AAV-GFP control virus (white bars) or with an uninjected control group ($n = 9$) (black bars) over a time course of 3 months following injection **(A).** The ERG a-wave and b-wave amplitudes of the *RHO301*-treated group were significantly elevated relative to GFP-injected or uninjected eyes at all time points (*$p < 0.05$ at 1 and 2 months post injection; **$p < 0.005$ at 3 months post injection). **(B)** AAV-*RHO301* protects the retina for up to 6 months. The a-wave and b-wave amplitudes of injected right eyes were elevated (white bars) in nine P23H transgenic mice at 1, 2, 3, and 6 months following injection, compared with uninjected left eyes (black bars) (*$p < 0.05$ at 1 and 2 months post injection; **$p < 0.005$ at 3 and 6 months). **(C)** Representative waveforms of P23H transgenic mice in uninjected eyes (left panel) and AAV-*RHO301*-injected eyes (right panel). **(D)** The scotopic ERG response in six P23H-*RHO* line 3 rats injected with AAV-*RHO301* in their right eyes (white bars). A 54% increase in a-wave amplitude relative to control uninjected left eyes (black bars) and a 27% increase in b-wave amplitude were observed in *RHO301*-injected P23H-*RHO* rats at 2 months post injection (*$p < 0.05$).

at the 6-month time point. At this stage, untreated eyes demonstrated less than 20% of the b-wave amplitude of the 1-month time point. In contrast, the P23H eyes treated with AAV-*RHO301* injection maintained 80% of the b-wave response compared with their amplitudes at 1 month. For sake of illustration, representative ERG waveforms from treated and untreated eyes of P23H mice are shown in Fig. 2C. This experiment demonstrated that the decline in retinal function in P23H transgenic mice was dramatically reduced by delivery of functional *RHO*.

To determine if the therapeutic effect of *RHO* delivery is limited to a single mouse model, we performed a pilot project in which we injected transgenic rats expressing P23H-*RHO* (line 3) with AAV-*RHO301*. This is a well characterized model of ADRP caused by *RHO* mutation (Organisciak *et al*., 2003; Lin *et al*., 2007). At 2 months post injection, gene transfer of *RHO301* to photoreceptors resulted in an increase in ERG a-wave and b-wave amplitudes in this ADRP model as well (Fig. 2D).

AAV-RHO301 *delivery damages wild-type retinas*

Overexpression of wild-type rhodopsin can be detrimental in transgenic mice (Olsson *et al*., 1992; Tan *et al*., 2001). To determine if overexpression of rhodopsin from viral delivery damaged the retinas of wild-type mice, we injected AAV-*RHO301* in C57BL/6J mice, which accumulate more rhodopsin than the P23H transgenic mice (Noorwez *et al*., 2009). Proteins were also extracted from wild-type C57BL/6J mice retinas 1 month after subretinal injection, and expression of rhodopsin was detected by anti-rhodopsin monoclonal antibody 1D4. There was a 45% increase in the monomer form of rhodopsin and a twofold increase in the dimer form in the *RHO301*-injected eyes compared with uninjected eyes ($p < 0.05$) (Supplementary Fig. S4). From 1 month to 6 months post treatment, both a-wave and b-wave amplitudes remained constant in the control eyes (Fig. 3A). However, by 1 month post injection, delivery of *RHO301* led to a slight (15%) reduction of the a-wave response. By 2 months after injection, the a-wave amplitude in *RHO301*-injected eyes dropped to half the value of that in untreated eyes. At 3 and 6 months post injection, the a-wave amplitude dropped at a slower rate. *RHO301* gene transfer led to a similar decline of b-wave amplitudes. The b-wave peaks were gradually reduced to 80% and 70% after 1 and 2 months post injection, whereas at 3 and 6 months post injection, the b-wave response remained at 33% of the untreated amplitude (Fig. 3A). In contrast to the P23H transgenic mice, wild-type mice had longer implicit time in ERG a-wave after *RHO301* injection in right eyes compared with left untreated wild-type eyes (Supplementary Fig. S3B).Therefore, injection with AAV-expressing normal rhodopsin reduced retinal function in wild-type mice. For illustration, wave forms of the treated and untreated ERG responses are presented in Fig. 3B.

AAV-RHO301 *preserves retinal structure in P23H mice*

The thickness of the ONL was measured as a metric of surviving photoreceptors in both the superior and inferior retinas of the P23H mice (Fig. 4A and B). Although the distribution of the ONL measurements showed regional differences between superior and inferior, there was better survival of photoreceptors after *RHO301* treatment of P23H

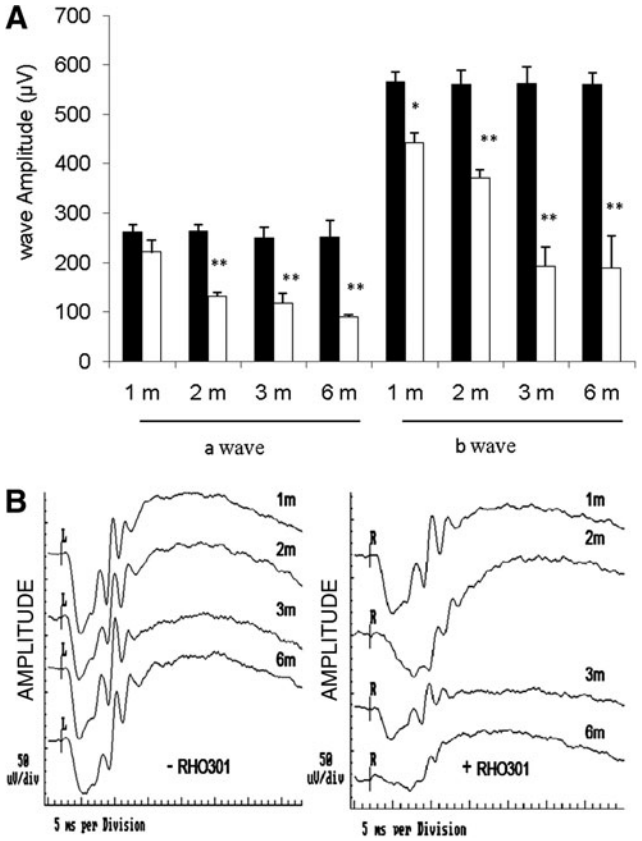

FIG. 3. AAV-*RHO*301delivery impairs the function of wild-type retinas. (**A**) Retinal degeneration was observed in seven wild-type mice injected with AAV5-*RHO301* by a reduction in both a-wave and b-wave amplitudes in injected right eyes (white bars) compared with the uninjected contralateral eyes (black bars) over a time course of 6 months. For the a-wave amplitudes, $^{**}p < 0.005$ at 2, 3, and 6 months post injection. For b-wave amplitudes, $^{*}p < 0.05$ at 1 month and $^{**}p < 0.005$ at 2, 3, and 6 months post injection. (**B**) ERG wave forms from wild-type mice either uninjected (left panel) or injected with AAV-*RHO301* (right panel).

transgenic mice, with approximately double the ONL thickness in most regions of the retina (Fig. 4E). Moreover, the thickness of the ONL from *RHO301* expression was remarkably elevated in the inferior retina close to the optic nerve head: $42.5 \pm 3.3\,\mu$m in *RHO301*-treated P23H eyes compared with the ONL thickness of $23.8 \pm 7.5\,\mu$m in untreated eyes ($p < 0.005$). Averaging across the entire retina, ONL thickness was 80% greater in *RHO301*-treated P23H eyes than in untreated P23H degenerated eyes (Fig. 4F). Higher magnification micrographs also showed longer and more normal appearing rod outer segments in *RHO301*-treated retinas compared with untreated control retinas (Supplementary Fig. S5). This difference was statistically significant ($p < 0.05$) in both the superior and inferior posterior retina. Increased length of rod outer segments is consistent with the increased rhodopsin content we measured immunologically (Fig. 1).

In contrast, in wild-type mice treated with *RHO301*, the ONL was thinner compared with that of control eyes (Fig. 4C and D). Although some superior and inferior regions had no significant changes, almost 40% reduction was detected in

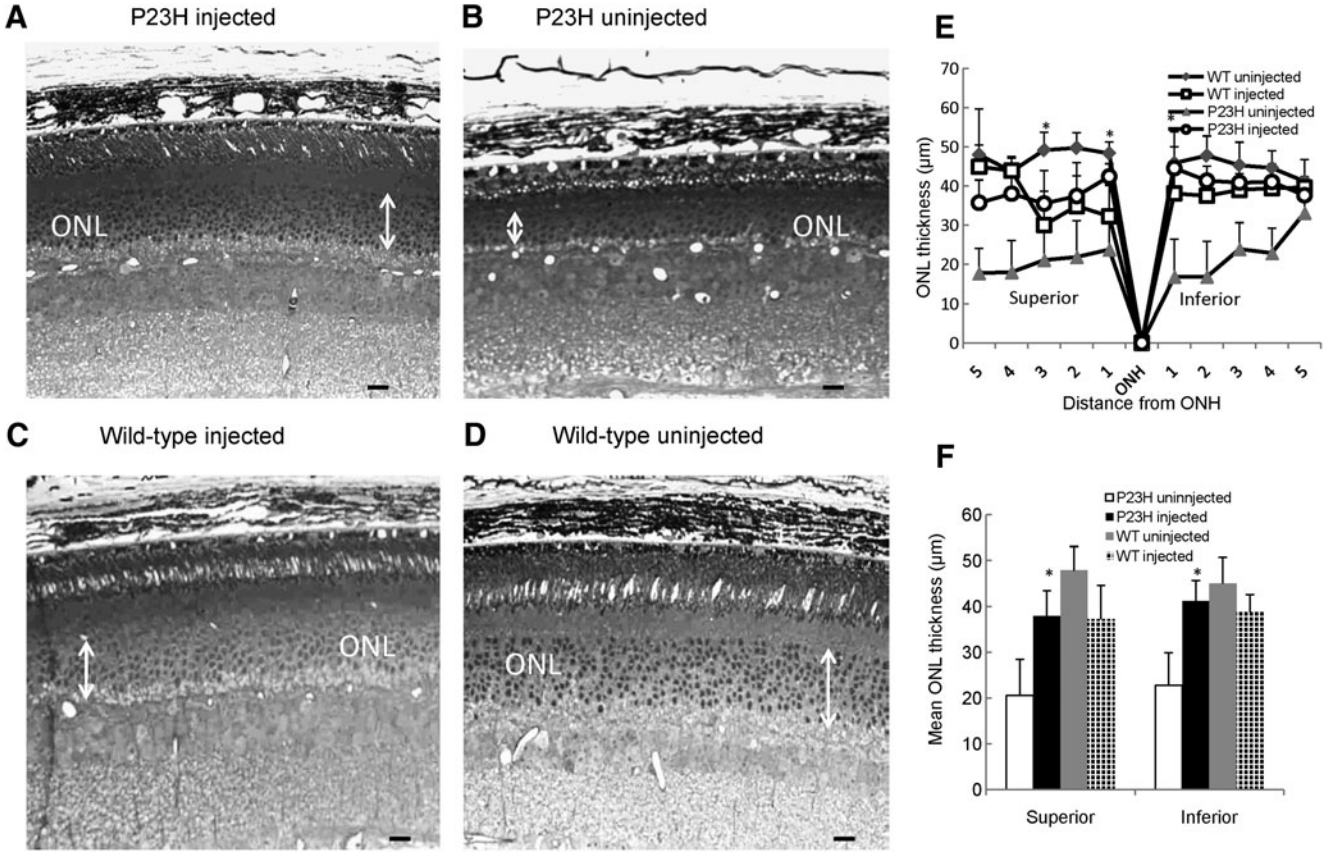

FIG. 4. *RHO301* gene delivery preserves the structural integrity of P23H retinas. The thickness of the ONL was measured in *RHO301*-injected P23H retinas (**A**) and compared with untreated contralateral retinas (**B**) from the same four mice at 6 months post injection. At most sites along the vertical meridian, the thickness of the ONL was greater in the *RHO301*-treated retinas. In contrast, the ONL from the *RHO301*-injected wild-type retinas (**C**) was thinner than that of untreated wild-type retinas (**D**). Calibration bar is 20 μm. Analysis was made as described by Lewin *et al*. (1998). Data are summarized from P23H mice and wild-type mice (**E**). Significant increase of the ONL thickness was detected in the *RHO301*-injected (right) eyes of P23H mice (circles) compared with the ONL of untreated (left) eyes (triangles) of the same animals (*$p < 0.05$ in the inferior retina). The ONL thickness in the *RHO301*-injected (right) retinas of wild-type mice (squares) was significantly reduced compared with the uninjected contralateral eyes (rectangles) (*$p < 0.05$ in the superior retina) (**E**). (**F**) Averaged data with overall ONL thickness from the same animal groups shown as a bar graph in both superior and inferior areas. For the P23H mice, both superior and inferior ONL from *RHO301*-injected retinas (black bars) were significantly thicker than that of the left untreated group (white bars) (*$p < 0.05$). In contrast, wild-type mice showed significant decrease in the ONL thickness only in the inferior area of the *RHO301*-injected eyes (small grid bars) compared with the uninjected wild-type eyes (gray bars) (*$p < 0.05$).

the central superior regions. The ONL thickness dropped from 48.3 ± 2.9 μm (central superior) and 49.2 ± 3.8 μm (central inferior) to 32.3 ± 7.9 μm and 30.0 ± 11.0 μm, respectively ($p < 0.05$) (Fig. 4E) (Faktorovich *et al*., 1990).

AAV delivery of RHO301 *reduced apoptosis in P23H mice*

To determine if increased ONL thickness was caused by suppression of apoptosis in P23H transgenic mice, we performed a nucleosome release assay using retinas 1 month following unilateral injection of AAV-*RHO301*. Apoptosis was reduced by 25% in injected eyes compared with that in uninjected eyes ($p < 0.05$) (Supplementary Fig. S6). This result was consistent with the rescued function of *RHO301*-injected retinas indicated by improvement in the ERG response and by preservation of retinal structure measured by increased ONL thickness (Figs. 2 and 4 and Supplementary Fig. S5).

Discussion

Frederick and colleagues determined that retinal degeneration was slower in P23H transgenic mice in the presence of two copies of the mouse *RHO* gene than in the presence of a single copy, suggesting that damage to photoreceptors is mitigated by increasing the ratio of wild-type/mutant rhodopsin (Frederick *et al*., 2001). We have converted their result into an application for gene therapy using viral delivery of wild-type *RHO*. We used AAV5 to transfer a gene encoding wild-type rhodopsin to P23H *RHO* transgenic mice to test the hypothesis that supplementation with functional rhodopsin would reduce the rate of photoreceptor demise. One month post injection, we observed a twofold increase of total *RHO* mRNA in treated eyes and a 58% increase in the monomer form of rhodopsin (Fig. 1). As we routinely obtain 70% transduction of the mouse retina following subretinal injection with AAV5, the rhodopsin increase might have been even greater on a per cell basis. The elevation in

rhodopsin synthesis that we observed was sufficient to preserve photoreceptors and maintain their function in P23H *RHO* transgenic mice. At 6 months post treatment, P23H *RHO* mice had a twofold increase in a-wave amplitude and a sixfold increase in b-wave amplitude relative to that of untreated transgenic eyes (Fig. 2) and corresponding to a 1.8-fold increase in survival of photoreceptors in the central retina of treated eyes (Fig. 4). This level of photoreceptor survival did not reach that of age-matched wild-type (C57BL/6) eyes, but we injected on P15 and, using single-stranded AAV, we could not expect vigorous expression of rhodopsin before 1 month of life. Based on the ERG amplitudes, delivery of *RHO* arrests the progression of the disease at about this stage. In contrast, the overexpression of normal rhodopsin in the retinas of wild-type mice led to a progressive reduction of scotopic ERG amplitudes between 1 month and 6 months post injection (Fig. 3). The damage to retinal structure was more substantial in the superior hemisphere, which is where we directed our injection (Fig. 4).

At this stage in our experiments, we cannot propose a precise mechanism for photoreceptor rescue by augmentation of rhodopsin synthesis in P23H rodents. In the absence of wild-type rhodopsin, P23H opsin accumulates in the ER and stimulates the unfolded protein response, leading to apoptosis (Lin *et al*., 2007; Gorbatyuk *et al*., 2010). However, in the presence of normal rhodopsin, some P23H rhodopsin traffics to the outer segment (Frederick *et al*., 2001). Increased expression of wild-type rhodopsin did not substantially affect markers of ER stress, such as GrP78 and CHOP (data not shown), but elevation of wild-type rhodopsin suppresses apoptosis (Supplementary Fig. S6). Even though rhodopsin is thought to be active as a monomer, it is organized as a lattice of dimers within the disc membranes of rod outer segments (Fotiadis *et al*., 2003). Consequently, we speculate that the P23H rhodopsin in the outer segment may interfere with function of normal rhodopsin, and the proportion of wild-type and mutant rhodopsin therefore determines the function and the stability of rod photoreceptors. This hypothesis was previously advanced by Wilson and Wensel (2003).

Tan *et al*. (2001) demonstrated that even modest overexpression of rhodopsin in transgenic mice can lead to retinal degeneration. In their experiments and those of Olsson *et al*. (1992), rhodopsin overexpression occurred during development of the retina, whereas our gene-delivery approach increased rhodopsin expression in mature photoreceptors. The question then arises: how much rhodopsin expression is too much? We found that an increase in rhodopsin expression was damaging to wild-type photoreceptors, but was protective to photoreceptors bearing the P23H transgene on the same background. However, the level of rhodopsin protein in the P23H transgenic mice is much lower than that in C57Bl/6 mice (Noorwez et al., 2009). As even wild-type opsin can misfold and aggregate, it is not surprising that a little extra is too much.

The most promising aspect of our results is that gene transfer of *RHO* may be applicable to other rhodopsin mutations that lead to RP by mechanisms similar to the P23H mutation. These include the largest class of *RHO* mutations that affect opsin folding and transport (Mendes *et al*., 2005). Therefore, the increase of rhodopsin expression by wild-type gene delivery is a potential treatment for a large fraction of ADRP patients. Human clinical trials of gene therapy for a recessive retinal degeneration have shown promise in restoring vision (Bainbridge *et al*., 2008; Cideciyan *et al*., 2009; Simonelli *et al*., 2010) and suggest that gene transfer to the retina is safe. Because of the toxicity of excess rhodopsin expression in wild-type mice (Fig. 4), a precise understanding of the dose response is required before *RHO* gene transfer should be attempted, and the response may depend on the amount of rhodopsin produced by the patient.

Acknowledgments

This work was supported by grant (TA-GT-0507-0384) from the Foundation Fighting Blindness and by the Vision Core Grant (NEI P30 08571) from the National Eye Institute. It was also supported by the Shaler Richardson Professorship endowment.

Author Disclosure Statement

William Hauswirth and the University of Florida own equity in AGTC, Inc., which could commercialize some aspect of this work.

References

Bainbridge, J.W.B., Smith, A.J., Barker, S.S., *et al*. (2008). Effect of gene therapy on visual function in Leber's congenital amaurosis. N. Engl. J. Med. 358, 2231–2239.

Bok, D. (2007). Contributions of genetics to our understanding of inherited monogenic retinal diseases and age-related macular degeneration. Arch. Ophthalmol. 125, 160–164.

Cashman, S.M., Binkley, E.A., and Kumar-Singh, R. (2005). Towards mutation-independent silencing of genes involved in retinal degeneration by RNA interference. Gene Ther. 12, 1223–1228.

Cideciyan, A.V., Hauswirth, W.W., and Aleman, T.S., *et al*. (2009). Human RPE65 gene therapy for Leber congenital amaurosis: persistence of early visual improvements and safety at 1 year. Hum. Gene Ther. 20, 999–1004.

Daiger, S.P., Bowne, S.J., and Sullivan, L.S. (2007). Perspective on genes and mutations causing retinitis pigmentosa. Arch. Ophthalmol. 125, 151–158.

Dryja, T.P., McGee, T.L., Reichel, E., *et al*. (1990). A point mutation of the rhodopsin gene in one form of retinitis pigmentosa. Nature 343, 364–366.

Dryja, T.P., McEvoy, J.A., McGee, T.L., and Berson, E.L. (2000). Novel rhodopsin mutations Gly114Val and Gln184Pro in dominant retinitis pigmentosa. Invest. Ophthalmol. Vis. Sci. 41, 3124–3127.

Faktorovich, E.G., Steinberg, R.H., Yasumura, D., *et al*. (1990). Photoreceptor degeneration in inherited retinal dystrophy delayed by basic fibroblast growth-factor. Nature 347, 83–86.

Farrar, G.J., Kenna, P.F., and Humphries, P. (2002). On the genetics of retinitis pigmentosa and on mutation-independent approaches to therapeutic intervention. EMBO J. 21, 857–864.

Flannery, J.G., Zolotukhin, S., Vaquero, M.I., *et al*. (1997). Efficient photoreceptor-targeted gene expression in vivo by recombinant adeno-associated virus. Proc. Natl. Acad. Sci. U.S.A. 94, 6916–6921.

Fotiadis, D., Liang, Y., Filipek, S., *et al*. (2003). Atomic-force microscopy: rhodopsin dimers in native disc membranes. Nature 421, 127–128.

Frederick, J.M., Krasnoperova, N.V., Hoffmann, K., *et al*. (2001). Mutant rhodopsin transgene expression on a null background. Invest. Ophthalmol. Vis. Sci. 42, 826–833.

Galy, A., Roux, M.J., Sahel, J.A., *et al*. (2005). Rhodopsin maturation defects induce photoreceptor death by apoptosis: a fly

model for Rhodopsin^{Pro23His} human retinitis pigmentosa. Hum. Mol. Genet. 14, 2547–2557.

Gorbatyuk, M., Justilien, V., Liu, J., *et al*. (2007a). Preservation of photoreceptor morphology and function in P23H rats using an allele independent ribozyme. Exp. Eye Res. 84, 44–52.

Gorbatyuk, M., Justilien, V., Liu, J., *et al*. (2007b). Suppression of mouse rhodopsin expression in vivo by AAV mediated siRNA delivery. Vision Res. 47, 1202–1208.

Gorbatyuk, M.S., Pang, J., Hauswirth, W., and Lewin, A. (2004). Ribozyme knockdown of endogenous mouse rhodopsin by AAV-delivered ribozymes. Invest. Ophthalmol. Vis. Sci. 45, U518–U518.

Gorbatyuk, M.S., Pang, J.J., Thomas, J., *et al*. (2005a). Knockdown of wild-type mouse rhodopsin using an AAV vectored ribozyme as part of an RNA replacement approach. Mol. Vis. 11, 648–656.

Gorbatyuk, M.S., Timmers, A.M.M., Pang, J.J., *et al*. (2005b). Rescue of vision in P23H rats with an rAAV delivered ribozyme targeting mouse opsin. Invest. Ophthalmol. Vis. Sci. 46, 4692.

Gorbatyuk, M.S., Hauswirth, W.W., and Lewin, A.S. (2008). Gene therapy for mouse models of ADRP. Adv. Exp. Med. Biol. 613, 107–112.

Gorbatyuk, M.S., Knox, T., Lavail, M.M., *et al*. (2010). Restoration of visual function in P23H rhodopsin transgenic rats by gene delivery of BiP/Grp78. Proc. Natl. Acad. Sci. U.S.A. 107, 5961–5966.

Hartong, D.T., Berson, E.L., and Dryja, T.P. (2006). Retinitis pigmentosa. Lancet 368, 1795–1809.

Illing, M.E., Rajan, R.S., Bence, N.F., and Kopito, R.R. (2002). A rhodopsin mutant linked to autosomal dominant retinitis pigmentosa is prone to aggregate and interacts with the ubiquitin proteasome system. J. Biol. Chem. 277, 34150–34160.

Kiang, A.S., Palfi, A., Ader, M., *et al*. (2005). Toward a gene therapy for dominant disease: validation of an RNA interference-based mutation-independent approach. Mol. Ther. 12, 555–561.

Laemmli, U.K. (1970). Cleavage of structural proteins during the assembly of the head of bacteriophage T4. Nature 227, 680–685.

Lewin, A.S., Drenser, K.A., Hauswirth, W.W., *et al*. (1998). Ribozyme rescue of photoreceptor cells in a transgenic rat model of autosomal dominant retinitis pigmentosa. Nat. Med. 4, 967–971.

Lewis, M.R., and Kono, M. (2006). Rhodopsin deactivation is affected by mutations of Tyrl91. Photochem. Photobiol. 82, 1442–1446.

Lin, J.H., Li, H., Yasumura, D., *et al*. (2007). IRE1 signaling affects cell fate during the unfolded protein response. Science 318, 944–949.

Mendes, H.F., van der Spuy, J., Chapple, J.P., and Cheetham, M.E. (2005). Mechanisms of cell death in rhodopsin retinitis pigmentosa: implications for therapy. Trends Mol. Med. 11, 177–185.

Noorwez, S.M., Sama, R.R.K., and Kaushal, S. (2009). Calnexin improves the folding efficiency of mutant rhodopsin in the presence of pharmacological chaperone 11-*cis*-retinal. J. Biol. Chem. 284, 33333–33342.

Olsson, J.E., Gordon, J.W., Pawlyk, B.S., *et al*. (1992). Transgenic mice with a rhodopsin mutation (Pro23His): a mouse model of autosomal dominant retinitis-pigmentosa. Neuron 9, 815–830.

O'Reilly, M., Millington-Ward, S., Palfi, A., *et al*. (2008). A transgenic mouse model for gene therapy of rhodopsin-linked retinitis pigmentosa. Vision Res. 48, 386–391.

Organisciak, D.T., Darrow, R.A., Barsalou, L., *et al*. (2003). Susceptibility to retinal light damage in transgenic rats with rhodopsin mutations. Invest. Ophthalmol. Vis. Sci. 44, 486–492.

Palfi, A., Ader, M., Kiang, A.S., *et al*. (2006). RNAi-based suppression and replacement of *rds*-peripherin in retinal organotypic culture. Hum. Mutat. 27, 260–268.

Phelan, J.K., and Bok, D. (2000). A brief review of retinitis pigmentosa and the identified retinitis pigmentosa genes. Mol. Vis. 6, 116–124.

Roof, D.J., Adamian, M., and Hayes, A. (1994). Rhodopsin accumulation at abnormal sites in retinas of mice with a human P23H rhodopsin transgene. Invest. Ophthalmol. Vis. Sci. 35, 4049–4062.

Saito, Y., Ohguro, H., Ohguro, I., *et al*. (2008). Misregulation of rhodopsin phosphorylation and dephosphorylation found in P23H rat retinal degeneration. Clin. Ophthalmol. 2, 821–828.

Simonelli, F., Maguire, A.M., Testa, F., *et al*. (2010). Gene therapy for Leber's congenital amaurosis is safe and effective through 1.5 years after vector administration. Mol. Ther. 18, 643–650.

Smith, A.J., Bainbridge, J.W., and Ali, R.R. (2009). Prospects for retinal gene replacement therapy. Trends Genet. 25, 156–165.

Stojanovic, A., Hwang, I., Khorana, H.G., and Hwa, J. (2003). Retinitis pigmentosa rhodopsin mutations L125R and A164V perturb critical interhelical interactions: new insights through compensatory mutations and crystal structure analysis. J. Biol. Chem. 278, 39020–39028.

Sullivan, J.M., Pietras, K.M., Shin, B.J., and Misasi, J.N. (2002). Hammerhead ribozymes designed to cleave all human rod opsin mRNAs which cause autosomal dominant retinitis pigmentosa. Mol. Vis. 8, 102–113.

Tam, B.M., and Moritz, O.L. (2006). Characterization of rhodopsin P23H-induced retinal degeneration in a *Xenopus laevis* model of retinitis pigmentosa. Invest. Ophthalmol. Vis. Sci. 47, 3234–3241.

Tan, E., Wang, Q., Quiambao, A.B., *et al*. (2001). The relationship between opsin overexpression and photoreceptor degeneration. Invest. Ophthalmol. Vis. Sci. 42, 589–600.

Tessitore, A., Parisi, F., Denti, M.A., *et al*. (2006). Preferential silencing of a common dominant rhodopsin mutation does not inhibit retinal degeneration in a transgenic model. Mol. Ther. 14, 692–699.

Timmers, A.M., Zhang, H., Squitieri, A., and Gonzalez-Pola, C. (2001). Subretinal injections in rodent eyes: effects on electrophysiology and histology of rat retina. Mol. Vis. 7, 131–137.

Van Soest, S., Westerveld, A., De Jong, P.T.V.M., *et al*. (1999). Retinitis pigmentosa: defined from a molecular point of view. Surv. Ophthalmol. 43, 321–334.

Wen, R., Song, Y., Cheng, T., *et al*. (1995). Injury-induced upregulation of bFGF and CNTF mRNAs in the rat retina. J. Neurosci. 15, 7377–7385.

Wilson, J.H., and Wensel, T.G. (2003). The nature of dominant mutations of rhodopsin and implications for gene therapy. Mol. Neurobiol. 28, 149–158.

Zolotukhin, S., Potter, M., Zolotukhin, I., *et al*. (2002). Production and purification of serotype 1, 2, and 5 recombinant adeno-associated viral vectors. Methods 28, 158–167.

Address correspondence to:
Dr. Alfred S. Lewin
University of Florida
P.O. Box 100266
Gainesville, FL 32610-0266

E-mail: Lewin@ufl.edu

Received for publication July 9, 2010;
accepted after revision November 30, 2010.

Published online: December 2, 2010.